

Article

Biochar as an Effective Filler of Carbon Fiber Reinforced Bio-Epoxy Composites

Danuta Matykiewicz 

Institute of Materials Technology, Faculty of Mechanical Engineering, Poznan University of Technology, Piotrowo 3, 61-138 Poznań, Poland; danuta.matykiewicz@put.poznan.pl

Received: 23 May 2020; Accepted: 17 June 2020; Published: 22 June 2020



Abstract: The goal of this work was to investigate the effect of the biochar additive (2.5; 5; 10 wt.%) on the properties of carbon fiber-reinforced bio-epoxy composites. The morphology of the composites was monitored by scanning electron microscopy (SEM), and the thermomechanical properties by dynamic mechanical thermal analysis (DMTA). Additionally, mechanical properties such as impact strength, flexural strength and tensile strength, as well as the thermal stability and degradation kinetics of these composites were evaluated. It was found that the introduction of biochar into the epoxy matrix improved the mechanical and thermal properties of carbon fiber-reinforced composites.

Keywords: composites; biochar; epoxy; carbon fiber

1. Introduction

The increase in the consumption of raw materials obtained from non-renewable resources is affecting the growing popularity of natural-origin materials. In addition, the circular economy, widely implemented by the European Union, requires that the design of polymer materials should result in a minimum impact on the natural environment [1]. Among the natural additives for polymers, plant, animal and mineral origin can be distinguished. They may occur in the form of powder, microparticles or nanoparticles, or long and short fibers [2–4]. The use of such modifiers as biochar [5–7], carbon nanotubes [8–10], basalt powder [11–14], lignin [15,16], and ground waste from the agricultural [17–19] and food industries [20–22] in polymer composites has been the subject of many scientific papers in recent years. A significant change in the properties of the polymer matrix is obtained by using additives of various shapes in the form of particles and fibers. Therefore, fiber-reinforced epoxy composites undergo modification with various bio-fillers in order to form hybrid materials [23]. Dinesh et al. [24] described the effects of wood dust, such as Rosewood and Padauk, on the properties of jute fiber/epoxy composites. The introduction of this filler has improved the mechanical and thermal properties of epoxy materials. In turn, *Azadirachta indica* seed powder, *Camellia sinensis* powder and their combinations have been used to modify epoxy resin reinforced with jute fabrics [25]. Epoxy composites with kenaf fiber and modified with various nanofillers—nano palm oil, empty bunch of fruit filler, montmorillonite, and organically modified montmorillonite—have also been studied [26]. The effect of *Pongamia pinnata* seed cake waste on the dry sliding wear behavior of basalt fabric-reinforced epoxy composites was examined by Mohan et al. [27]. Moreover, micro rice husk powder and rice husk ash powder have also been applied to improve the flexural strength and the fatigue life of the carbon fabric/epoxy composites [28].

Biocarbon is a porous solid obtained through the thermal decomposition of biomass. It is chemically stable under ambient conditions [29]. Biochar properties depend mainly on the raw material and on the pyrolysis temperature used in the production process [30]. The thermal stability of the biochar results from the high pyrolysis temperature, which usually exceeds 350 °C. In addition, it can have functional groups on its surfaces, which facilitate its connection with the polymer matrix [31]. Bartoli et al. [32]

studied the effect of the addition of biochar with different morphologies on the properties of epoxy composites. In another study [30], biochar was used to modify the electrical characteristics of epoxy composites. The application of pure and high-temperature annealed biochar to enhance the mechanical behaviors of epoxy materials was presented by Giorcelli et al. [33]. The introduction of biochar obtained from different feedstock (rice husk, oil seed rape, softwoods, perennial rhizomatous cane, wheat straw), pyrolyzed under the same conditions in order to improve the ductility of the epoxy resin, has also been analyzed [34]. Additionally, biocarbons from Chinese Poplar and pine cones have been successfully applied to improve the elastic behaviors of epoxy materials [35]. Savi et al. [36] showed that the tensile properties of epoxy composites modified with 4 wt.% multi wall carbon nanotubes and 20 wt.% maple wood biochar were similar. All of these reports have demonstrated the high application potential of biocarbon as an additive to epoxy materials.

Polymer composites reinforced with carbon fiber show good chemical resistance and mechanical properties at a low density [37]. Therefore, the introduction of a bio additive that can both reduce their price and improve their properties is a desirable product solution. To the best of the author's knowledge, the use of biocarbon to modify the properties of carbon fiber-reinforced epoxy composites has not yet been reported in the literature. Hence, the goal of this work was to investigate the impact of the biochar additive on the properties of carbon fiber-reinforced bio-epoxy composites. The present paper presents the results of a study into the structure, dynamic mechanical thermal behavior, mechanical properties such as flexural strength, impact strength and tensile strength, as well as thermal stability and degradation kinetics of these composites.

2. Materials and Methods

2.1. Materials

The structural composites were made using: high biobased content epoxy resin (37%) SuperSap ONE (Entropy resin), hardener SuperSap ONS (Entropy resin), and plain carbon fabric SPREAD, areal weight 160 g/m² (ECC). The mixing ratio of resin and hardener recommended by the producer was 100:47 (by weight) or 2:1 (by volume). Biochar (BC) (Fluid SA, Sędziszów) from biomass (mainly willows) was used in the pyrolysis process at 650 °C, and then crushed in a ball mill for 24 h, using steel balls as a filler. The biochar production process is repeatable and always takes place in repetitive and controlled conditions, and its properties can be closely related to the type of biomass.

2.2. Preparation of Composites

In the first stage, biochar was introduced into the epoxy resin in amounts of 2.5, 5, and 10 weight percent, using a high shear mixer (10 min/1000 rpm). Next, the compositions were combined with the hardener (5 min/500 rpm). The mixture was then degassed for 15 min under a pressure of −0.8 bar and used for laminating the carbon fabric layers. Using a hand lay-up technique, the composites containing six layers of carbon fabric were made, and then cured for 7 days at 23 °C and for 3 h at 80 °C. The samples were described as 0 BC; 2.5 BC; 5 BC; and 10 BC, in reference to their biocarbon (BC) content. The composite production scheme is presented in Figure 1.

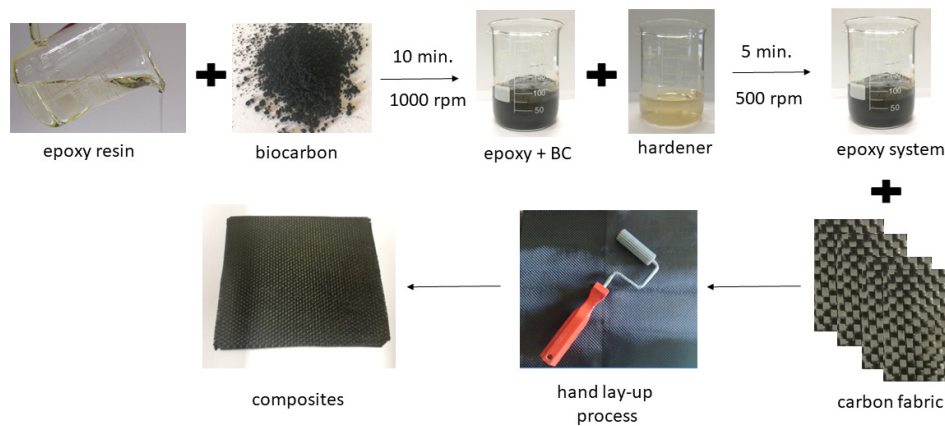


Figure 1. Preparation of epoxy/carbon fiber composites modified with biocarbon.

2.3. Methods

2.3.1. Scanning Electron Microscopy (SEM)

Scanning electron microscopy (SEM) was used to assess the morphology of the composites and biocarbon. The structure of biocarbon was monitored at the magnification of 6000 and 20,000, while the fracture surfaces of the composites were studied at the enlargement of 1000, and then recorded digitally by a scanning electron microscope Zeiss Evo 40 (Oberkochen, Germany) with an electron accelerating voltage of 12 kV. Before testing, all of the samples were sprayed with a layer of gold.

2.3.2. Dynamic Mechanical Thermal Analysis (DMTA)

Dynamic mechanical thermal analysis was used to determine the thermomechanical properties of the composites, such as: the storage modulus (G'), the glass transition temperature (T_g) and the damping factor ($\tan \delta$). Measurements were made in the torsion mode (Anton Paar MCR 301 apparatus) with a frequency of 1 Hz, in the temperature range from 25 to 150 °C, with a heating rate of 2 °C/min. As a point for determining the value of the glass transition temperature (T_g), the maximum $\tan \delta$ value was selected.

2.3.3. Flexural Test

A three-point bending test (Zwick Roell Z010 testing machine) was conducted for 80 mm × 10 mm × 2.0 mm samples with DIN EN ISO 14125. The measuring speed was 1 mm/min, and the load cell was 10 kN. The span length corresponded to 16 times the sample thickness.

2.3.4. Charpy Impact Strength

The impact strength of the unnotched samples was tested by the Charpy method (ISO 179) at room temperature. In addition, the peak load as the maximum force (F_{max}) was determined during the test. A Zwick/Roell HIT 25P impact tester with a 5 J hammer was used.

2.3.5. Tensile Test

The tensile test of the composites was carried out using an INSTRON 4481 universal testing machine according to ISO 527-4, at 25 °C, with a test speed of 1 mm/min and a load cell of 50 kN.

2.3.6. Thermogravimetry (TGA)

The thermal properties of the composites were determined by thermogravimetry (TGA) in an atmosphere of nitrogen and air, in a temperature range from 30 to 900 °C and a heating rate of 10 °C/min (Netzsch TG 209 F1 apparatus). The samples with a mass of 10 mg were investigated in ceramic vessels. The following values were designated: the temperature at which the weight loss was 10% ($T_{10\%}$),

the residual mass at 900 °C (W%) and maximum thermal degradation temperatures from derivative thermogravimetric (DTG) diagrams. Moreover, according to the Kissinger method, TGA measurements were conducted in a nitrogen atmosphere at a heating rate of 5, 10, 15, 20 °C/min.

3. Results

3.1. Composites Structure

The morphology of biocarbon particles depends on the biomass from which it was produced and the method of its treatment. Biochar formed from organic biomass by pyrolysis can form a skeletal structure with macropores, mesopores or micropores. Particles of the ground biocarbon with an average diameter of 4–8 µm, obtained from deciduous trees, were characterized by a smooth and clean surface (Figure 2). Basalt fiber coverage by the epoxy matrix was observed for all tested samples. In the case of the biochar-modified composites, no filler agglomeration was observed, which may indicate a good connection between all the components (Figure 3). This is important because, as reported by [38], the mechanical interlocking of biochar in a polymer chain may result in improved mechanical properties of the composites.

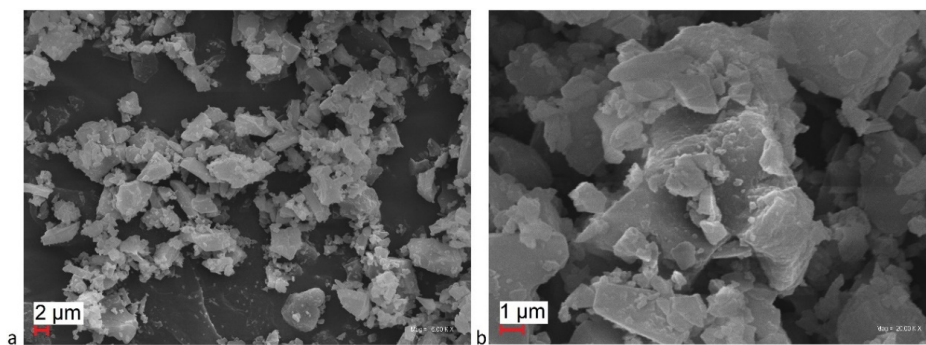


Figure 2. Structure of used biocarbon (a) magnification 6000×, (b) magnification 20000×.

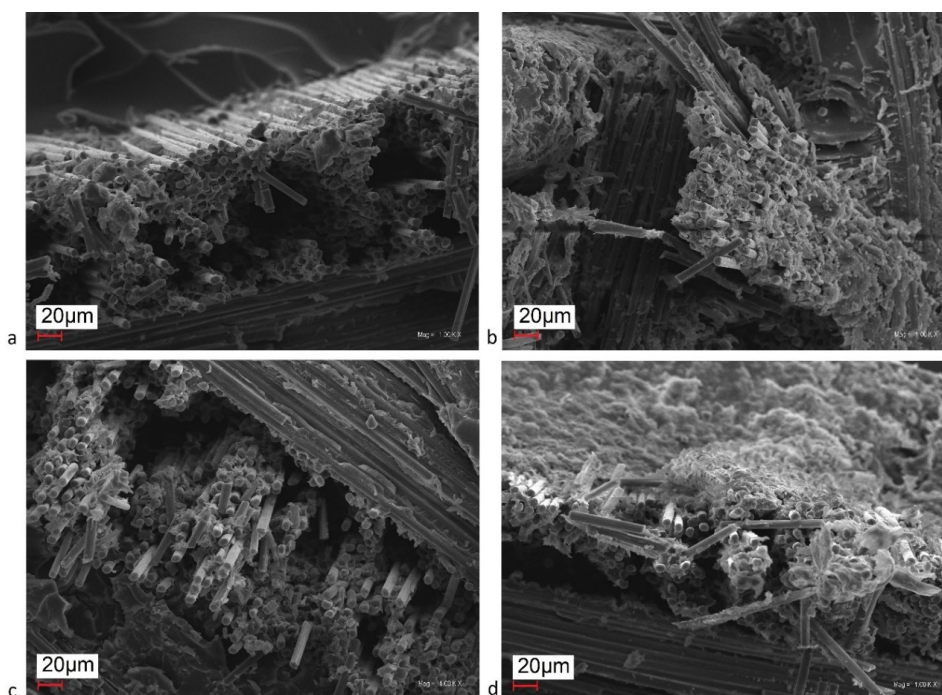


Figure 3. Structure of the composites (a) 0 BC, (b) 2.5 BC, (c) 5 BC, (d) 10 BC at a magnification of 1000×.

3.2. Thermomechanical Properties

DMTA analysis was performed to identify the effect of BC introduction into the epoxy matrix on the viscoelastic properties of the composites. Changes in the value of the storage modulus and damping factor are associated with the interaction between the polymer matrix, fiber and fillers (Table 1). Figure 4 presents the dependence of the storage modulus and damping factor on the temperature. The storage modulus values corresponding to the material stiffness increased with the increasing BC content [39]. The G' value began to decrease at a temperature above 50 °C and when it reached the glass transition temperature, it dropped significantly. The damping factor ($\tan \delta$) describes the relationship between the elastic and viscous phases in polymeric materials; the high $\tan \delta$ value is due to the high degree of energy dissipation (non-elastic deformation), while the low $\tan \delta$ value shows that the material is more elastic [40]. For all tested materials, $\tan \delta$ values and glass transition temperatures were similar and averaged 0.50 and 73 °C, respectively. These results are in good agreement with the study by Temmink et al. [41]. It should be emphasized that the addition of biochar improves the stiffness of the material without reducing its glass transition temperature, which is important because of the functional properties that this composite material should have.

Table 1. DMTA analysis data: storage modulus (G'), glass transition temperature (T_g) and damping factor ($\tan \delta$).

Sample	G' at 30 °C (MPa)	G' at 100 °C (MPa)	T_g (°C)	$\tan \delta$
0 BC	2150 ± 35	75.1 ± 3.5	73 ± 2	0.51 ± 0.2
2.5 BC	2720 ± 40	82.4 ± 2.5	73 ± 2	0.49 ± 0.3
5 BC	2810 ± 45	93.3 ± 3.0	71 ± 2	0.55 ± 0.1
10 BC	2990 ± 35	129.0 ± 3.0	73 ± 2	0.45 ± 0.2

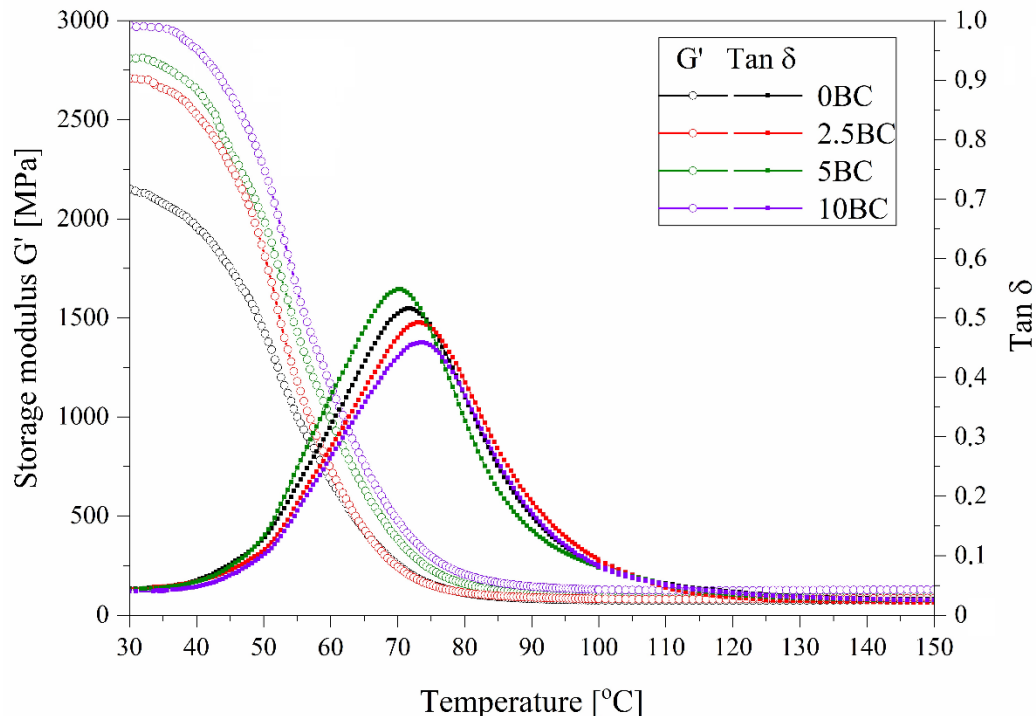


Figure 4. Graph of dependence of storage modulus (G') and damping factor ($\tan \delta$) values on temperature obtained by the DMTA.

3.3. Flexural Properties

In order to emphasize the impact of the addition of biochar on the flexural behavior of epoxy materials, flexural strength and modulus depending on the filler content are presented in Figure 5, and the data are also presented collectively in Table 2. The flexural strength of the composite depends mainly on the dispersion of the particles, and the wetting and infiltration of the polymer in the particles [42]. The flexural strength value increased with increasing biochar addition from 275 to 323 MPa. This may have been due to the presence of rigid biochar with a high surface area in the epoxy matrix. The value of the flexural modulus slightly decreased, which may have been a result of a lower amount of epoxy in the composites, in comparison with the reference sample. The increase in inorganic filler content caused an increase in the flexural modulus of the composites [43,44].

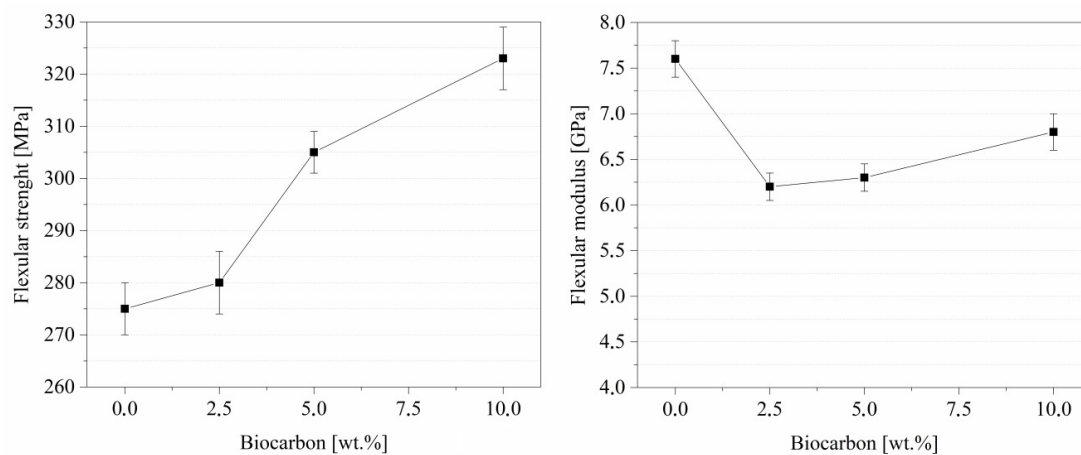


Figure 5. Flexural strength and modulus of the composites.

Table 2. Flexural and impact values of the tested materials.

Sample	Flexural Strength (MPa)	Flexural Modulus (GPa)	Impact Strength (kJ/m ²)	F _{max} (N)
0 BC	275 ± 2	7.6 ± 0.2	55.3 ± 0.8	183.9 ± 5.8
2.5 BC	280 ± 1	6.2 ± 0.15	65.5 ± 2.5	221.3 ± 4.1
5 BC	305 ± 2	6.3 ± 0.15	69.4 ± 0.7	210.2 ± 6.4
10 BC	323 ± 1	6.8 ± 0.2	72.7 ± 2.1	210.5 ± 9.1

3.4. Charpy Impact Strength

The impact strength and maximum force (peak load) values of the tested composites are collected in Table 2. During the impact test of the fiber-reinforced composites, f energy is dissipated by a combination of several phenomena, such as fiber pulling, fiber cracking, and matrix deformations and crack [45]. The increase in the biocarbon content in the epoxy matrix resulted in an increase in the impact strength of the composites. In addition, after the introduction of biocarbon into the epoxy, the laminates showed an increase in their peak load (F_{max}) from 183 to 221 N. This may indicate good adhesion between all the components of the biocomposites [46]. The typical load–time plots of the examined materials are presented in Figure 6. Based on the shape of the curves, it can be assumed that the destruction mechanism was similar in all cases, and that the addition of the powder filler did not cause voids that could act like notches in the structure of the composite.

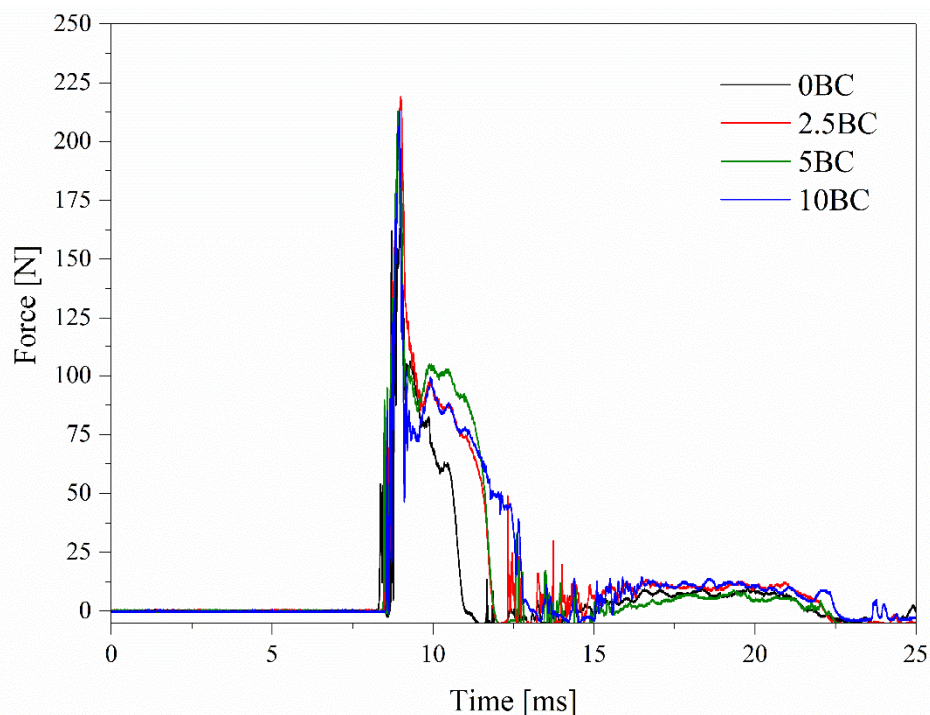


Figure 6. The load–time curves of the investigated composites.

3.5. Tensile Behaviours

In order to obtain more complete mechanical properties of the composites, a tensile test was carried out, and tensile strength, modulus of elasticity and elongation at break were determined (Table 3). The tensile strength value of fiber-reinforced polymer materials usually differs from their bending strength value. This is mainly due to the properties of the reinforcing fibers used, their structure, and weave. The tensile strength of the composites with the largest amount of biochar was similar to the reference sample. Moreover, for all of the modified composites, the tensile modulus value was lower than that of the unmodified composite. Meanwhile, for the 10 BC sample, this value was near to the value for 0 BC. The elongation at break was at the same level for all tested materials.

Table 3. Tensile test values of the tested materials.

Sample	Tensile Strength (MPa)	Tensile Modulus (GPa)	Elongation at Break (%)
0 BC	375 ± 5	16.6 ± 0.2	2.5 ± 0.2
2.5 BC	305 ± 4	13.5 ± 0.3	2.6 ± 0.1
5 BC	355 ± 2	14.3 ± 0.2	2.5 ± 0.2
10 BC	380 ± 3	15.5 ± 0.2	2.5 ± 0.3

3.6. Thermal Stability

The thermal stability of biochar and the composites was assessed by the thermogravimetric method in both an inert and oxidizing atmosphere. Characteristic thermogravimetric (TG) and DTG curves are shown in Figures 7–9, and data are collected in Tables 4 and 5. Biochar was thermally stable in a nitrogen atmosphere up to a temperature of 530 °C, at which 10% weight loss was observed and the residual mass was 83%. In the air atmosphere, a one-stage biocarbon decomposition was observed, and T10% value and residual mass were 396 °C and 4.9%, respectively.

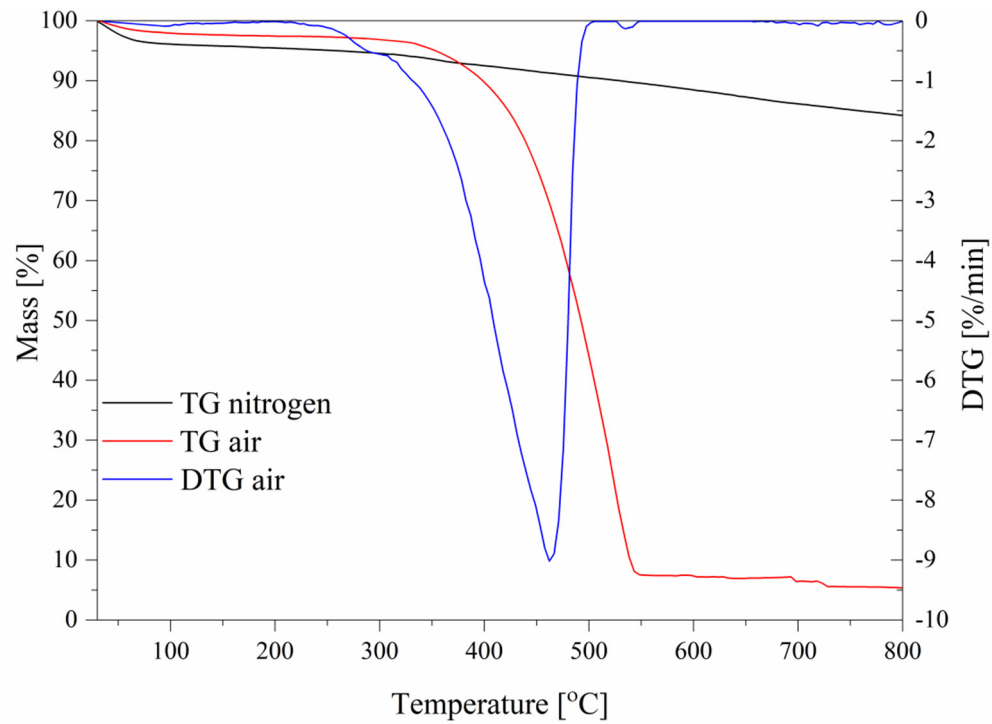


Figure 7. Thermogravimetric (TG) and derivative thermogravimetric (DTG) curves biocarbon under nitrogen and air atmosphere.

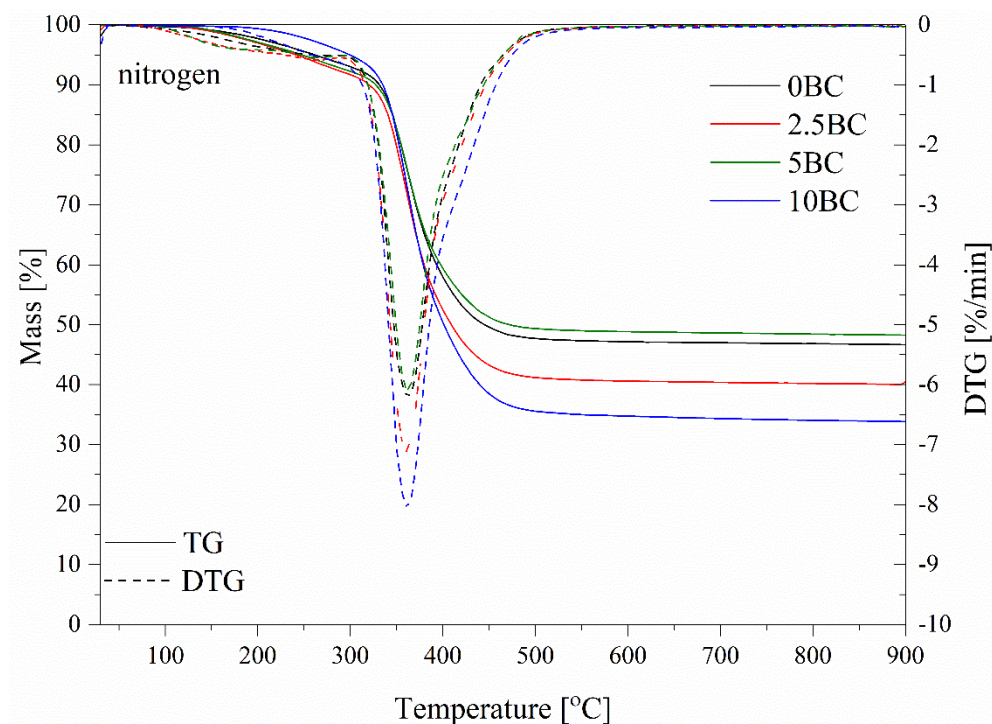


Figure 8. The diagrams of TG and DTG for analyzed materials obtained in a nitrogen atmosphere.

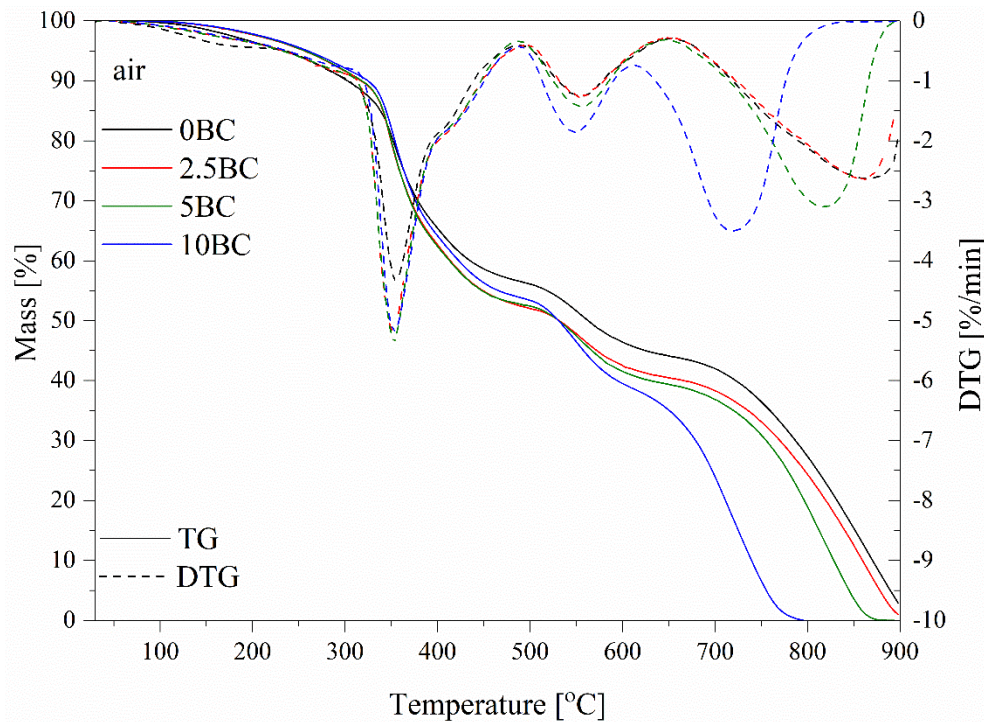


Figure 9. The diagrams of TG and DTG for analyzed materials obtained in air atmosphere.

Table 4. Results of thermogravimetry (TGA) analysis for composites and biochar examined in nitrogen atmosphere.

Name	T10% (°C)	Residual Mass (%)	DTG Peak Temperature (°C)	Max Degradation Rate (%/min)
BC	528.9	82.9	-	-
0 BC	329.5	45.57	355.6	6.22
2.5 BC	331.1	42.00	359.1	6.87
5 BC	329.0	42.89	360.2	7.04
10 BC	329.5	44.18	358.8	6.82

Table 5. Results of TGA analysis for composites and biochar examined in air atmosphere.

Name	T10% (°C)	Residual Mass (%)	DTG Peak Temperature (°C)	Max Degradation Rate (%/min)
BC	396.4	4.92	507.9	8.2
0 BC	302.6	1.0	345.1	4.98
2.5 BC	317.2	0.9	346.5	6.07
5 BC	318.3	0.5	350.2	5.68
10 BC	324.9	0.1	353.4	5.19

In the case of the composites tested in a nitrogen atmosphere, the addition of biochar did not significantly affect their thermal stability. A one-stage degradation process was observed for all the tested samples, T10% was, on average, 330 °C and the residual mass was 43–45% (Table 3). Another effect was observed for samples tested in the air atmosphere; the thermal stability of the composites increased along with the increase in biochar content in the epoxy matrix. The temperature at which a 10% weight loss of the examined materials was recorded increased from 302 to 325 °C, and the temperature from the DTG peak increased from 345 to 353 °C (Table 4). For the samples examined in the air atmosphere, a three-stage degradation process was observed. The first peak on the DTG curve occurred in the temperature range of 345–353 °C, corresponding to resin degradation, and the addition of biochar shifted this temperature to a higher value. The major peak associated with filler

oxidation at 508 °C was observed at the DTG biochar curve (Figure 7). Moreover, DTG peaks between 500 and 600 °C and above 650 °C were associated with the oxidation and degradation of biochar and carbon fibers.

In addition, in order to assess the effect of the addition of biochar on the thermal properties of the composites, TGA measurements were conducted at different heating rates, and the activation energy of degradation was determined based on the Kissinger method. This method takes into account the maximum temperatures (T_m) determined from DTG curves obtained at different heating rates (β) [47]. In this method, the peak of the DTG curve corresponds to the temperature at which the reaction rate has its maximum value. The activation energy, according to the Kissinger method, is described in the Equation (1):

$$\frac{d[\ln(\beta/T_m^2)]}{d(1/T_m^2)} = \frac{-E_a}{R} \quad (1)$$

where: E_a —activation energy; R —gas constant; β —heating rate; T_m —temperature of DTG peak.

In this method, the activation energy can be calculated from a plot of $\ln(\beta/T_m^2)$ versus $1/T_m$ (Figure 10). The values of E_a were assessed from the values of the slope coefficient of a straight line, described by Equation (2).

$$E_a = -\text{slope} \times R \quad (2)$$

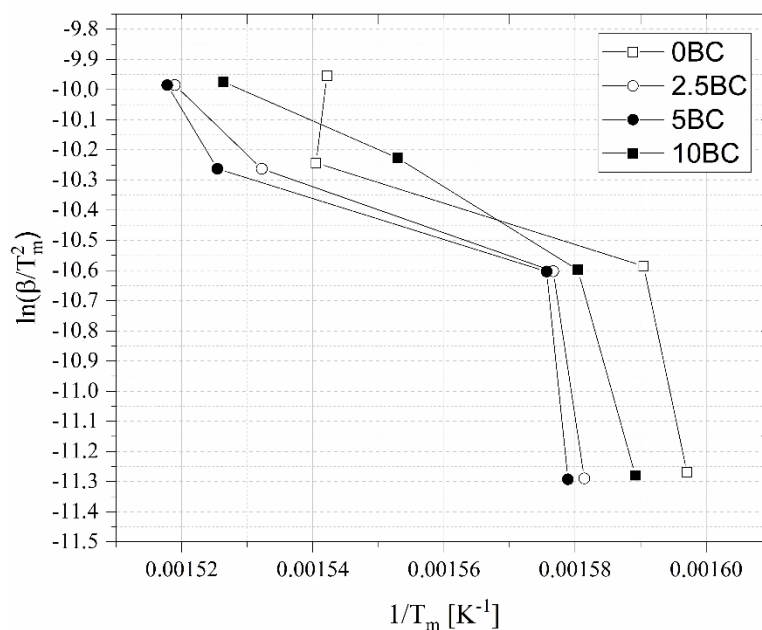


Figure 10. Kissinger plots of investigated composite in nitrogen.

The Kissinger method was employed to calculate the activation energy in nitrogen. The values of the activation energy E_a of the thermal degradation process, determined by the Kissinger method, and T_m obtained from DTG curves at different heating rates, are collected in Table 6. It was observed that as the heating temperature increased, the DTG value of the peak shifted to higher temperatures. This effect is caused by shortening the time until the sample reaches the same temperature, and the material does not manage to completely decompose, therefore resulting in the T_m values being higher [48]. For the composites with the highest biochar content, a significant increase in the E_a value was observed from 136 to 151 kJ/mol. It can be concluded that during the thermal degradation, the biochar additive may retard the thermal decomposition of the carbon fiber-reinforced composites.

Table 6. Kissinger data of investigated composite in nitrogen.

Name	T _p at 5 °C/min (°C)	T _p at 10 °C/min (°C)	T _p at 15 °C/min (°C)	T _p at 20 °C/min (°C)	Ea (kJ/mol)
0 BC	353.0 ± 2.0	355.6 ± 1.8	375.8 ± 2.1	375.3 ± 2.0	136.3 ± 2.2
2.5 BC	359.2 ± 1.8	361.1 ± 2.0	379.5 ± 1.7	385.2 ± 2.0	133.9 ± 3.0
5 BC	360.2 ± 2.5	361.5 ± 2.2	382.4 ± 1.9	385.7 ± 2.0	137.5 ± 1.9
10 BC	356.1 ± 2.1	359.6 ± 1.9	370.8 ± 2.1	382.0 ± 2.0	151.2 ± 2.0

4. Conclusions

In this work, biochar was successfully used as a low-cost filler in carbon fiber-reinforced epoxy composites. Due to its specific properties, the introduction of biochar to the epoxy matrix has contributed to the improvement of the thermomechanical properties of materials, such as storage modulus, and mechanical properties, such as flexural and impact strength. The composites containing the highest amount of filler, i.e., 10 wt.%, showed the most favorable properties. Moreover, thanks to the thermogravimetric method, it was confirmed that the introduction of biochar to the epoxy matrix improves the thermal stability of the composites and delays the process of their thermal degradation in the air atmosphere. In addition, the Kissinger method determined the activation energy of the thermal degradation process. The highest value was recorded for the composites containing 10 wt.% biochar. To sum up, the paper found a beneficial effect of using biochar in epoxy composites reinforced with carbon fibers, which confirms the usefulness of this carbon derivative as a modifier in polymeric materials.

Funding: This research was funded by the Ministry of Science & Higher Education in Poland under Project No 0613/SBAD/4630.

Conflicts of Interest: The authors declare no conflict of interest.

References

1. Czarnecka-Komorowska, D.; Wiszumirska, K. Sustainability design of plastic packaging for the Circular Economy. *Polimery* **2020**, *65*, 8–17. [[CrossRef](#)]
2. Hamad, Q.A.; Abed, M.S. Investigation of thyme and pumpkin nanopowders reinforced epoxy matrix composites. *J. Mech. Eng. Res. Dev.* **2019**, *42*, 153–157. [[CrossRef](#)]
3. Zaini, E.; Azaman, M.; Jamali, M.; Ismail, K. Synthesis and characterization of natural fiber reinforced polymer composites as core for honeycomb core structure: A review. *J. Sandw. Struct. Mater.* **2020**, *22*, 525–550. [[CrossRef](#)]
4. Oliwa, R.; Oliwa, J.; Bulanda, K.; Oleksy, M.; Budzik, G. Effect of modified bentonites on the crosslinking process of epoxy resin with aliphatic amine as curing agent. *Polimery* **2019**, *64*, 499–503. [[CrossRef](#)]
5. Andrzejewski, J.; Misra, M.; Mohanty, A.K. Polycarbonate biocomposites reinforced with a hybrid filler system of recycled carbon fiber and biocarbon: Preparation and thermomechanical characterization. *J. Appl. Polym. Sci.* **2018**, *135*, 1–14. [[CrossRef](#)]
6. Arrigo, R.; Jagdale, P.; Bartoli, M.; Tagliaferro, A.; Malucelli, G. Structure-property relationships in polyethylene-based composites filled with biochar derived from waste coffee grounds. *Polymers* **2019**, *11*, 1336. [[CrossRef](#)] [[PubMed](#)]
7. Gezahegn, S.; Lai, R.; Huang, L.; Chen, L.; Huang, F.; Blozowski, N.; Thomas, S.C.; Sain, M.; Tjong, J.; Jaffer, S.; et al. Porous graphitic biocarbon and reclaimed carbon fiber derived environmentally benign lightweight composites. *Sci. Total Environ.* **2019**, *664*, 363–373. [[CrossRef](#)]
8. Whulanza, Y.; Battini, E.; Vannozi, L.; Vomero, M.; Ahluwalia, A.; Vozzi, G. Electrical and Mechanical Characterisation of Single Wall Carbon Nanotubes Based Composites for Tissue Engineering Applications. *J. Nanosci. Nanotechnol.* **2013**, *13*, 188–197. [[CrossRef](#)]
9. Bekyarova, E.; Thostenson, E.T.; Yu, A.; Kim, H.; Gao, J.; Tang, J.; Hahn, H.T.; Chou, T.-W.; Itkis, M.E.; Haddon, R.C. Multiscale Carbon Nanotube–Carbon Fiber Reinforcement for Advanced Epoxy Composites. *Langmuir* **2007**, *23*, 3970–3974. [[CrossRef](#)]

10. He, Y.; Yang, S.; Liu, H.; Shao, Q.; Chen, Q.; Lu, C.; Jiang, Y.; Liu, C.; Guo, Z. Reinforced carbon fiber laminates with oriented carbon nanotube epoxy nanocomposites: Magnetic field assisted alignment and cryogenic temperature mechanical properties. *J. Colloid Interface Sci.* **2018**, *517*, 40–51. [[CrossRef](#)]
11. Barczewski, M.; Mysiukiewicz, O.; Matykiewicz, D.; Skórczewska, K.; Lewandowski, K.; Andrzejewski, J.; Piasecki, A. Development of polylactide composites with improved thermomechanical properties by simultaneous use of basalt powder and a nucleating agent. *Polym. Compos.* **2020**. [[CrossRef](#)]
12. Pavlović, M.; Dojčinović, M.; Prokić-Cvetković, R.; Andrić, L. Cavitation resistance of composite polyester resin/basalt powder. *Struct. Integr. Life* **2019**, *19*, 19–22.
13. Abusahmin, F.; Algellai, A.; Tomic, N.; Vuksanovic, M.; Majstorovic, J.; Volkov-Husovic, T.; Simic, V.; Jancic-Heinemann, R.; Toljic, M.; Kovacevic, J. Basalt-polyester hybrid composite materials for demanding wear applications. *Sci. Sinter.* **2020**, *52*, 67–76. [[CrossRef](#)]
14. Prasath, K.A.; Arumugaprabu, V.; Amuthakkannan, P.; Manikandan, V.; Deepak Joel Johnson, R. Low velocity impact, compression after impact and morphological studies on flax fiber reinforced with basalt powder filled composites. *Mater. Res. Express* **2019**, *7*. [[CrossRef](#)]
15. Gioia, C.; Colonna, M.; Tagami, A.; Medina, L.; Sevastyanova, O.; Berglund, L.A.; Lawoko, M. Lignin-Based Epoxy Resins: Unravelling the Relationship between Structure and Material Properties. *Biomacromolecules* **2020**. [[CrossRef](#)]
16. Klapiszewski, Ł.; Jamrozik, A.; Strzemieska, B.; Koltsov, I.; Borek, B.; Matykiewicz, D.; Voelkel, A.; Jesionowski, T. Characteristics of Multifunctional, Eco-Friendly Lignin-Al₂O₃ Hybrid Fillers and Their Influence on the Properties of Composites for Abrasive Tools. *Molecules* **2017**, *22*, 1920. [[CrossRef](#)]
17. Nagarajan, K.J.; Balaji, A.N.; Basha, K.S.; Ramanujam, N.R.; Kumar, R.A. Effect of agro waste α -cellulosic micro filler on mechanical and thermal behavior of epoxy composites. *Int. J. Biol. Macromol.* **2020**, *152*, 327–339. [[CrossRef](#)]
18. Kumar, R.; Bhowmik, S. Quantitative probing of static and dynamic mechanical properties of different bio-filler-reinforced epoxy composite under assorted constraints. *Polym. Bull.* **2020**. [[CrossRef](#)]
19. Salasinska, K.; Barczewski, M.; Borucka, M.; Górny, R.L.; Kozikowski, P.; Celiński, M.; Gajek, A. Thermal Stability, Fire and Smoke Behaviour of Epoxy Composites Modified with Plant Waste Fillers. *Polymers* **2019**, *11*, 1234. [[CrossRef](#)]
20. Mysiukiewicz, O.; Barczewski, M.; Skórczewska, K.; Szulc, J.; Kloziński, A. Accelerated Weathering of Polylactide-Based Composites Filled with Linseed Cake: The Influence of Time and Oil Content within the Filler. *Polymers* **2019**, *11*, 1495. [[CrossRef](#)]
21. Li, R.; Li, W.; Zheng, F.; Zhang, Y.; Hu, J. Versatile bio-based epoxy resin: From banana waste to applied materials. *J. Appl. Polym. Sci.* **2019**, *136*, 1–8. [[CrossRef](#)]
22. Mysiukiewicz, O.; Barczewski, M.; Szulc, J. The Influence of Poly(Vinyl Alcohol) on Oil Release Behavior of Polylactide- Based Composites Filled with Linseed Cake. *J. Renew. Mater.* **2020**, *8*, 347–363. [[CrossRef](#)]
23. Matykiewicz, D. Hybrid Epoxy Composites with Both Powder and Fiber Filler: A Review of Mechanical and Thermomechanical Properties. *Materials* **2020**, *13*, 1802. [[CrossRef](#)] [[PubMed](#)]
24. Dinesh, S.; Kumaran, P.; Mohanamurugan, S.; Vijay, R.; Singaravelu, D.L.; Vinod, A.; Sanjay, M.R.; Siengchin, S.; Bhat, K.S. Influence of wood dust fillers on the mechanical, thermal, water absorption and biodegradation characteristics of jute fiber epoxy composites. *J. Polym. Res.* **2020**, *27*, 9. [[CrossRef](#)]
25. Vijay, R.; Vinod, A.; Kathiravan, R.; Siengchin, S.; Singaravelu, D.L. Evaluation of Azadirachta indica seed/spent Camellia sinensis bio-filler based jute fabrics–epoxy composites: Experimental and numerical studies. *J. Ind. Text.* **2020**, *49*, 1252–1277. [[CrossRef](#)]
26. Saba, N.; Paridah Abdan, K.; Ibrahim, N.A. Dynamic mechanical properties of oil palm nano filler/kenaf/epoxy hybrid nanocomposites. *Constr. Build. Mater.* **2016**, *124*, 133–138. [[CrossRef](#)]
27. Mohan, N.; Ashok Kumar, R.; Rajesh, K.; Padmanaban, S.; Chetan, K.; Akshay Prasad, M. Investigation on Tribological Behaviour of Bio-Based Pongamia Pinnata Seed Cake Waste Incorporated Basalt Epoxy Composites. *Mater. Today Proc.* **2019**, *18*, 5309–5316. [[CrossRef](#)]
28. Nam, G.; Kim, J.; Song, J.-I. Mechanical Performance of Bio-Waste-Filled Carbon Fabric/Epoxy Composites. *Polym. Compos.* **2019**, *40*, E1504–E1511. [[CrossRef](#)]
29. Mahdian, M.; Huang, L.Y.; Kirk, D.W.; Jia, C.Q. Water permeability of monolithic wood biocarbon. *Microporous Mesoporous Mater.* **2020**, *303*, 110258. [[CrossRef](#)]

30. Giorcelli, M.; Savi, P.; Khan, A.; Tagliaferro, A. Analysis of biochar with different pyrolysis temperatures used as filler in epoxy resin composites. *Biomass Bioenergy* **2019**, *122*, 466–471. [[CrossRef](#)]
31. Ogunsona, E.O.; Codou, A.; Misra, M.; Mohanty, A.K. Thermally Stable Pyrolytic Biocarbon as an Effective and Sustainable Reinforcing Filler for Polyamide Bio-composites Fabrication. *J. Polym. Environ.* **2018**, *26*, 3574–3589. [[CrossRef](#)]
32. Bartoli, M.; Nasir, M.A.; Jagdale, P.; Passaglia, E.; Spiniello, R.; Rosso, C.; Giorcelli, M.; Rovere, M.; Tagliaferro, A. Influence of pyrolytic thermal history on olive pruning biochar and related epoxy composites mechanical properties. *J. Compos. Mater.* **2019**, *54*, 1863–1873. [[CrossRef](#)]
33. Giorcelli, M.; Khan, A.; Pugno, N.M.; Rosso, C.; Tagliaferro, A. Biochar as a cheap and environmental friendly filler able to improve polymer mechanical properties. *Biomass Bioenergy* **2019**, *120*, 219–223. [[CrossRef](#)]
34. Bartoli, M.; Giorcelli, M.; Rosso, C.; Rovere, M.; Jagdale, P.; Tagliaferro, A. Influence of commercial biochar fillers on brittleness/ductility of epoxy resin composites. *Appl. Sci.* **2019**, *9*, 3109. [[CrossRef](#)]
35. Oral, I. Determination of elastic constants of epoxy resin/biochar composites by ultrasonic pulse echo overlap method. *Polym. Compos.* **2016**, *37*, 2907–2915. [[CrossRef](#)]
36. Savi, P.; Jose, S.P.; Khan, A.A.; Giorcelli, M.; Tagliaferro, A. Biochar and carbon nanotubes as fillers in polymers: A comparison. In Proceedings of the 2017 IEEE MTT-S International Microwave Workshop Series on Advanced Materials and Processes for RF and THz Applications, Pavia, Italy, 20–22 September 2017. IMWS-AMP 2017.
37. Forintos, N.; Czigany, T. Multifunctional application of carbon fiber reinforced polymer composites: Electrical properties of the reinforcing carbon fibers—A short review. *Compos. Part B Eng.* **2019**, *162*, 331–343. [[CrossRef](#)]
38. Bowlby, L.K.; Saha, G.C.; Afzal, M.T. Flexural strength behavior in pultruded GFRP composites reinforced with high specific-surface-area biochar particles synthesized via microwave pyrolysis. *Compos. Part A Appl. Sci. Manuf.* **2018**, *110*, 190–196. [[CrossRef](#)]
39. Dahal, R.K.; Acharya, B.; Saha, G.; Bissessur, R.; Dutta, A.; Farooque, A. Biochar as a filler in glassfiber reinforced composites: Experimental study of thermal and mechanical properties. *Compos. Part B Eng.* **2019**, *175*, 107169. [[CrossRef](#)]
40. Chee, S.S.; Jawaid, M.; Sultan, M.T.H.; Alothman, O.Y.; Abdullah, L.C. Thermomechanical and dynamic mechanical properties of bamboo/woven kenaf mat reinforced epoxy hybrid composites. *Compos. Part B Eng.* **2019**, *163*, 165–174. [[CrossRef](#)]
41. Temmink, R.; Baghaei, B.; Skrifvars, M. Development of biocomposites from denim waste and thermoset bio-resins for structural applications. *Compos. Part A Appl. Sci. Manuf.* **2018**, *106*, 59–69. [[CrossRef](#)]
42. Das, O.; Bhattacharyya, D.; Hui, D.; Lau, K.-T. Mechanical and flammability characterisations of biochar/polypropylene biocomposites. *Compos. Part B Eng.* **2016**, *106*, 120–128. [[CrossRef](#)]
43. Mariotti, G.; Vannozzi, L. Fabrication, Characterization, and Properties of Poly (Ethylene-Co-Vinyl Acetate) Composite Thin Films Doped with Piezoelectric Nanofillers. *Nanomaterials* **2019**, *9*, 1182. [[CrossRef](#)] [[PubMed](#)]
44. Cafarelli, A.; Losi, P.; Salgarella, A.R.; Barsotti, M.C.; Di Cioccio, I.B.; Foffa, I.; Vannozzi, L.; Pingue, P.; Soldani, G.; Ricotti, L. Small-caliber vascular grafts based on a piezoelectric nanocomposite elastomer: Mechanical properties and biocompatibility. *J. Mech. Behav. Biomed. Mater.* **2019**, *97*, 138–148. [[CrossRef](#)] [[PubMed](#)]
45. Wambua, P.; Ivens, J.; Verpoest, I. Natural fibres: Can they replace glass in fibre reinforced plastics? *Compos. Sci. Technol.* **2003**, *63*, 1259–1264. [[CrossRef](#)]
46. Fiore, V.; Sanfilippo, C.; Calabrese, L. Influence of sodium bicarbonate treatment on the aging resistance of natural fiber reinforced polymer composites under marine environment. *Polym. Test.* **2019**, *80*, 106100. [[CrossRef](#)]
47. Kissinger, H.E. Reaction Kinetics in Differential Thermal Analysis. *Anal. Chem.* **1957**, *29*, 1702–1706. [[CrossRef](#)]
48. Jiao, C.; Zhang, C.; Dong, J.; Chen, X.; Qian, Y.; Li, S. Combustion behavior and thermal pyrolysis kinetics of flame-retardant epoxy composites based on organic–inorganic intumescent flame retardant. *J. Therm. Anal. Calorim.* **2015**, *119*, 1759–1767. [[CrossRef](#)]

